AIMETA 2019
XXIV Conference
The Italian Association of Theoretical and Applied Mechanics
Rome, Italy, 15–19 September 2019

MULTIPLE CRACK LOCALIZATION AND DEBONDING MECHANISMS FOR THIN THERMAL COATING FILMS

Guido Borino[1] **and Francesco Parrinello**[2]

[1] Università di Palermo, Department of Engineering
Viale delle Scienze 90128 Ed.8, 90128 Palermo, Italy
e-mail: guido.borino@unipa.it

[2] Università di Palermo, Department of Engineering
Viale delle Scienze 90128 Ed.8, 90128 Palermo, Italy
e-mail: francesco.parrinello@unipa.it

Keywords: Strain localization, Interface, Debonding, Nonlocal Damage, Coating Spalling off.

Abstract. *Experimental tests, carried out on small scale alloy specimens covered on one side with a thin thermal coating, have shown complex failure mechanisms. The failure mechanisms observed are due to the competition between two fracture mechanisms. The two mechanisms are: (i) Vertical tensile coating surface cracks and (ii) debonding shear decohesion mechanisms along the interface between the coating and the substrate. The present paper analyzes the mechanical problem of the nonlinear behavior thin film on a stiff substrate adopting a computational approach. Namely, incremental 2D nonlinear finite element simulations. The stiff superalloy substrate is modeled as a thermo-elastic material. The coating film is constitutively modeled as quasibrittle material with a nonlocal elastic-damage constitutive relation. The formation and propagation of cracks between the coating film and the superalloy substrate is modeled by a zero-thickness cohesive-frictional mechanical interface. Finite Element results are analyzed with respect to the distance between the surface cracks and the debonding at the interface coating/substrate. A final consideration on the influence of the thickens of the coating is discussed.*

1 INTRODUCTION

Experimental tensile tests carried out on small scale specimens covered on one external side with a thin thermal coating, used as thermal barrier to a superalloy structural substrate, have shown complex failure mechanisms [1, 2, 3].

The dominating failure mechanisms observed are due to the competition between two fracture mechanisms. First, the formation, on the external coating surface, of vertical tensile cracks, which grows in number and propagates in the interior of the coating up to reach the substrate interface. Then, the tensile opening cracks can pass through the interface or, more likely, a debonding shear mechanism may develops along the interface between the coating (typically a ceramic-type material with quasibrittle constitutive behavior) and the high strength superalloy substrate.

The final failure mechanism shows the fragmentation, with subsequent expulsion of small pieces the coating barrier film, which leave the superalloy undercoated and then exposed to the very high temperature variations.

Very high temperature variations can be dangerous not only for the development of high thermal strains, but mostly for possible solid phase changes induced in the superalloy.

Analytical results are available only assuming simplified conditions such as full adhesion between the two materials and uniaxial state of stress, obtain closed form relation for the mutual distance between adjacent vertical surface cracks [1]. A further insight for evaluating the debonding development along the interface can be achieved adopting an analytical approach similar to the one proposed by Alessi et al. [4]. A complete picture of all the involved nonlinear mechanisms requires numerical approaches.

The present paper analyzes the mechanical problem of the nonlinear behavior thin film on a stiff substrate adopting a computational approach. Namely, incremental 2D nonlinear Finite Element simulations are adopted, modeling the stiff superalloy as a thermo-elastic material.

The coating layers are generally realized with materials with high thermal insulation properties such as ceramic materials. These materials under high stress conditions behave as quasibrittle. Namely as the elastic limit stress condition is reached, damage in the form of initial microcracks start to nucleate. From a constitutive point of view nonlocal elastic-damage constitutive relation is a rational modeling choice [5].

The nonlocality feature in the elastic-damage model allow to reproduce the formation of damage localization in a mesh-objective way.

The formation and propagation of cracks between the coating film and the superalloy substrate is modeled by a zero-thickness cohesive-frictional mechanical interface [6, 7, 8, 9].

Nonlocal damage and interface interactions has been previously proposed in [10] for the analysis of FRP reinforcement to quasibrittle substrate. Competition between interface and and regularized brittle fracture by phase filed approach has been investigated in [11]

The overall formulation has been implemented in an open source nonlinear finite element program and a number of 2D simulations have been carried out.

A discussion on the amplitude and on the relative distance between the surface cracks is presented. The correlation between mechanical properties of the materials and of the interface, together with the influence of the thickens of the coating are analyzed.

2 SUBSTRATE AND COATING LAYER

The analysis is carried out on a specimen that reproduces a typical tension test. Namely one end is fixed and the other is subjected to an imposed uniform displacement $\bar{u}$ The specimen of length L is composed by two materials: i) the superalloy substrate of thickness H_{sub} and the thermal coating of thickness h_{rc}. The problem under consideration is treated in plain strain condition. Detail are reported in Figure. 1.

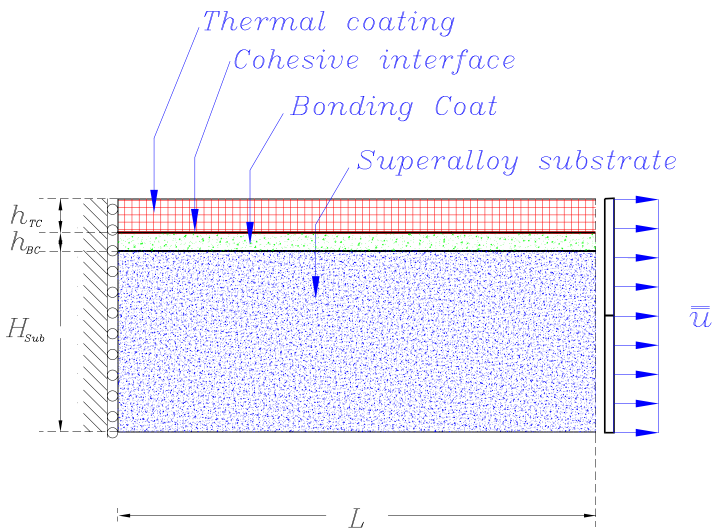

Figure 1: Specimen composed by an elastic superalloy substrate and a quasi-brittle thermal coating. The two layers are connected by a mechanical cohesive-frictional interface which embeds the properties of the bonding coat.

The substrate is a superalloy which by hypothesis responds following the linear elasticity law along the entire loading history.

The coating is usually composed of materials with high thermal insulation properties, such as ceramics, which can be modeled by an elastic-quasibrittrle constitutive law. Continuum damage models can be adopted for modeling the response of the coating layer, since they can reproduce the elastic degradation of the material up to the formation and propagation of localized cracks. Namely, damage models at same stage turn in the softening regime, which is responsible of localization of strains. As the damage approach unity the localized strain can be considered a physical crack. Strain localization is a source of theoretical and computational troubles and, in order to maintain mesh objective results, regularization techniques are required such as: non-local damage models [12, 5], gradient damage models [13], or following more recent trends, phase field approaches [14].

In between the substrate and the thermal coating layer a bond coating very thin film is inserted, which could be a Ni foil. This film is introduced as a primer for an higher adhesion between the two materials and also as an efficient barrier against the corrosion of the superalloy, [15]. The bonding layer has a very small thickness and is the locus where under the action of shear and normal laminar stress the delamination mechanism may develop. For this reason it is modeled as a zero thickness cohesive frictional mechanical interface. The mechanical interface models are very popular for modeling cohesive fracture problems, with special emphasis when the locus of possible formation and propagation of the fracture is known a-priori. There is a vast literature on interface mechanical models ([6, 16, 7, 17, 18])

2.1 The nonlocal damage model for the coating

The ceramic thermal coating mechanically behaves as a quasi-brittle material, therefore a nonlocal damage model appears to be appropriate.

The model adopted is a symmetric formulation thermodynamically consistent based on the formulation proposed in [5]. The nonlocal aspect allows to introduce in the constitutive formulation an internal length parameter ℓ which takes into account the effect of the microstructure dimension into the spatial spread of the damage band. Nonlocal damage is then able to predict strain localization of a finite thickness related to the material microstructure and therefore the relevant size effect.

The relation between the Cauchy stress tensor and the infinitesimal strain tensor is given as

$$\boldsymbol{\sigma}(\boldsymbol{x}) = \big(1 - \bar{\omega}(\boldsymbol{x})\big)\, \boldsymbol{E}\, \boldsymbol{\varepsilon}(\boldsymbol{x}) \tag{1}$$

where $\boldsymbol{\sigma}$ is the Cauchy stress tensor, $\boldsymbol{E}$ is the material elastic moduli tensor, $\boldsymbol{\varepsilon}$ is the infinitesimal strain tensor and $\bar{\omega}$ is a nonlocal measure of the isotropic scalar damage space distribution ω. Namely, $\bar{\omega}$ is a space weight average of the local damage ω obtained as

$$\bar{\omega}(\boldsymbol{x}) = \int_V W(\boldsymbol{x}, \boldsymbol{y})\, \omega(\boldsymbol{y})\, dV(\boldsymbol{y}) \tag{2}$$

The spatial weight function $W(\boldsymbol{x}, \boldsymbol{y})$ is given as

$$W(\boldsymbol{x}, \boldsymbol{x}) = \left(1 - \frac{\Omega_r(\boldsymbol{x})}{\Omega_\infty}\right) \delta(\boldsymbol{x}, \boldsymbol{y}) + \frac{1}{\Omega_\infty} \exp\left(-\frac{||\boldsymbol{x} - \boldsymbol{y}||^2}{2\ell^2}\right) \tag{3}$$

The spatial weight function W defined in eq.(3) results as a sum of two parts. The first part is a local contribution which produces effects at points close (with respect to the internal length ℓ) to the boundary of the body V and tend to vanish for points far from the boundary. $\delta(\boldsymbol{x})$ being the Dirac delta function. The second part is characterized by a positive decreasing kernel, here an exponential function in which the decreasing rate depends on the relative distance $r = ||\boldsymbol{x} - \boldsymbol{y}||$ and on the internal length parameter ℓ. This second part becomes dominant for points of the body far from the boundary of V. The function Ω_r is a measure of the dimension of the nonlocal interaction domain and is defined as

$$\Omega_r(\boldsymbol{x}) = \int_V \exp\left(-\frac{||\boldsymbol{x} - \boldsymbol{y}||^2}{2\ell^2}\right) dV(\boldsymbol{y}) \tag{4}$$

When points are far from the boundary the above quantity becomes a constant Ω_∞ which is the finite value of the integral given in eq.(4) when the integration is performed over the unbounded 2D domain. The weighting function W, defined in eq.(3), is symmetric with respect to $\boldsymbol{x}, \boldsymbol{y}$ at any point in V and satisfy the following normality condition:

$$\int_V W(\boldsymbol{x}, \boldsymbol{y})\, dV(\boldsymbol{y}) = 1. \tag{5}$$

Beside the constitutive relation (1) a nonlocal damage activation function is defined as

$$\phi_d(\bar{Y}, \chi) = \bar{Y} - \chi - Y_0 \leq 0 \tag{6}$$

where

$$\bar{Y}(\boldsymbol{x}) = \int_V W(\boldsymbol{x}, \boldsymbol{y})\, Y(\boldsymbol{y})\, dV(\boldsymbol{y}) \tag{7}$$

where Y is the energy release rate, χ is an internal variable able to characterize the post peak stress-strain softening material response and Y_0 is the initial damage activation threshold.

$$Y = \frac{1}{2} \boldsymbol{\varepsilon}^T \boldsymbol{E}\, \boldsymbol{\varepsilon} \tag{8}$$

Following a damage softening law proposed by Comi and Perego, [19], the internal variable χ is related to the damage ω by the following state law

$$\chi = \kappa \ln^n \left(\frac{c}{1-\omega} \right) - \kappa \ln^n c \tag{9}$$

where κ, n, c are parameters that describes the post elastic stress-strain response. With reference to the uni-axial response it is possible to identify the constitutive constants by the following relations ([19])

- Damage threshold: $Y_0 \equiv 1/2 E \varepsilon_e^2 = \kappa \ln^n c$
- Fracture Energy $G_f = Y_0 + cn\kappa \exp[-(Y_0/\kappa)^{1/n}](n-1)! \sum(1/i!)(Y_0/\kappa)^{i/n}$

The constant $c \geq 1$ is related to the stress-strain slope at the final elastic strain ε_e, and for $c = e^{n/2}$ an initial horizontal slope is achieved followed by negative slope, i.e. softening.

The nonlocal damage constitutive framework is then completed by the following damage flow rules and the loading/unloading conditions:

$$\dot{\omega} = \frac{\partial \phi_d}{\partial \bar{Y}} \dot{\lambda} = -\frac{\partial \phi_d}{\partial \chi} \dot{\lambda} \tag{10}$$

$$\dot{\lambda} \geq 0, \qquad \phi_d \leq 0, \qquad \dot{\lambda} \phi_d = 0. \tag{11}$$

2.2 The cohesive-frictional interface model

In order to describe the development of discontinuities in the displacement at the bounding region between the substrate and the thermal coating layer (debonding) a mechanical interface is introduced. The interface model adopted for the analysis is a recent evolution of a thermodynamically consistent mixed-mode cohesive-frictional interface model developed by the authors [8, 9, 20, 21].

The interface model is based on the assumption that the dechoesion surface can be decomposed in two fractions related to the value of a surface damage variable ω_s. Namely, a creaked fraction $\omega_s\, dS$ and a sound fraction $(1-\omega_s)\, dS$. The traction vector $\boldsymbol{t}$ across the interface is therefore given as a sum of the two contributions $\boldsymbol{t} = \boldsymbol{t}_s + \boldsymbol{t}_c$ with

$$\boldsymbol{t}_s = (1-\omega_s) \boldsymbol{K}_s \boldsymbol{\delta}_s^e; \qquad \boldsymbol{t}_c = \omega_s \boldsymbol{K}_c \boldsymbol{\delta}_c^e \tag{12}$$

where $\boldsymbol{K}_s$ and $\boldsymbol{K}_c$ are the diagonal stiffness matrices of the two interface fraction and $\boldsymbol{\delta}_s^e$ and $\boldsymbol{\delta}_c^e$; are respectively the interface displacement discontinuity vectors for the two fractions. Two activation functions are introduced for the description of mode I (opening), mode II (sliding) and any mixed mode. The first is a damage activation function:

$$\phi_d^s = Y_s - \chi_s - \tilde{Y}_{s0}(\boldsymbol{u}) - Y_{s0} \leq 0 \tag{13}$$

where Y_{s0} is the initial threshold for the surface damage activation, χ_s is the internal variable that drives the interface softening state and finally $\tilde{Y}_{s0}(\boldsymbol{u})$ is a positive term which allows to drive fracture mixity. Y_s is the surface energy release rate given as

$$Y_s = \frac{1}{2} \boldsymbol{\delta}_s^{eT} \boldsymbol{K}_s \boldsymbol{\delta}_s^e - \frac{1}{2} \boldsymbol{\delta}_c^{eT} \boldsymbol{K}_c \boldsymbol{\delta}_c^e \tag{14}$$

A second activation function is introduced, which takes into account the frictional behavior in the form of a Mohr-Coulomb yield function

$$\phi_p^s(\boldsymbol{t}_c) = |t_{ct}| + \alpha t_{cn} \leq 0 \tag{15}$$

where α is the frictional coefficient and t_{ct} and t_{cn} are the tangential and normal components of the traction vector $\boldsymbol{t}_c$ which acts on the damaged fraction and can generate frictional effects even before that the interface is fully damaged. The interface damage flow rule reads

$$\dot{\omega}_s = \frac{\partial \phi_d^s}{\partial \bar{Y}_s} \dot{\lambda}_s = -\frac{\partial \phi_d^s}{\partial \chi_s} \dot{\lambda}_s \tag{16}$$

and regarding the frictional displacements

$$\dot{\delta}_n^p = \frac{\partial \psi_p}{\partial t_{cn}} \dot{\lambda}_p = sgn(t_{ct})\dot{\lambda}_p \qquad \dot{\delta}_t^p = \frac{\partial \psi_p}{\partial t_{ct}} \dot{\lambda}_p = \beta \dot{\lambda}_p \tag{17}$$

where ψ_p is the interface frictional potential given as

$$\psi_p(\boldsymbol{t}_c) = |t_{ct}| + \beta t_{cn} \tag{18}$$

in which $\beta \leq \alpha$ is the dilatancy coefficient.

The damage interface constitutive formulation is finally completed by the loading unloading conditions

$$\dot{\lambda}_s \geq 0, \quad \phi_d^s \leq 0, \quad \dot{\lambda}_s \phi_d^s = 0; \qquad \dot{\lambda}_p \geq 0, \quad \phi_p^s \leq 0, \quad \dot{\lambda}_p \phi_p^s = 0; \tag{19}$$

3 NUMERICAL APPLICATION

The constitutive relations described in the previous Sections has been implemented in the open source finite element code FEAP. The nonlinear analysis has been conducted on the structural element of Fig. 1. The domain has been discretized by 9-node plane strain elements, whereas along the boundary between the two materials 6-node interface elements have been used. The length of the specimen is $L = 10$ mm. The thickness of the substrate is $H_{sub} = 1.5$ mm. Two different thickness for the thermal coating layer has been considered. The first is a thin coating $h_{rc}^{(1)} = 0.2$ mm, whereas the second is a thick coating of $h_{rc}^{(2)} = 0.6$ mm.

The substrate is considered as an isotropic linear elastic material with elastic modulus $E_s =$ 200 GPa and Poisson ration $\nu_s = 0.3$

The thermal coating has been considered as a nonlocal elastic damage material following the model of Sec. 2.1. The material data adopted are:

- Elastic modulus $E_c = 25$ GPa
- Poisson ratio $\nu_c = 0.3$
- Damage parameters $c = 2.7182$; $\kappa = 0.018$; $n = 2$.
- damage internal length $\ell = 0.02$ mm

The potential dechoesion mechanisms between the substrate and the thermal coating is modeled by zero-thickness cohesive-frictional 6-node interface elements. The constitutive model described in Sec. 2.2. has been implemented with the following constitutive parameters:

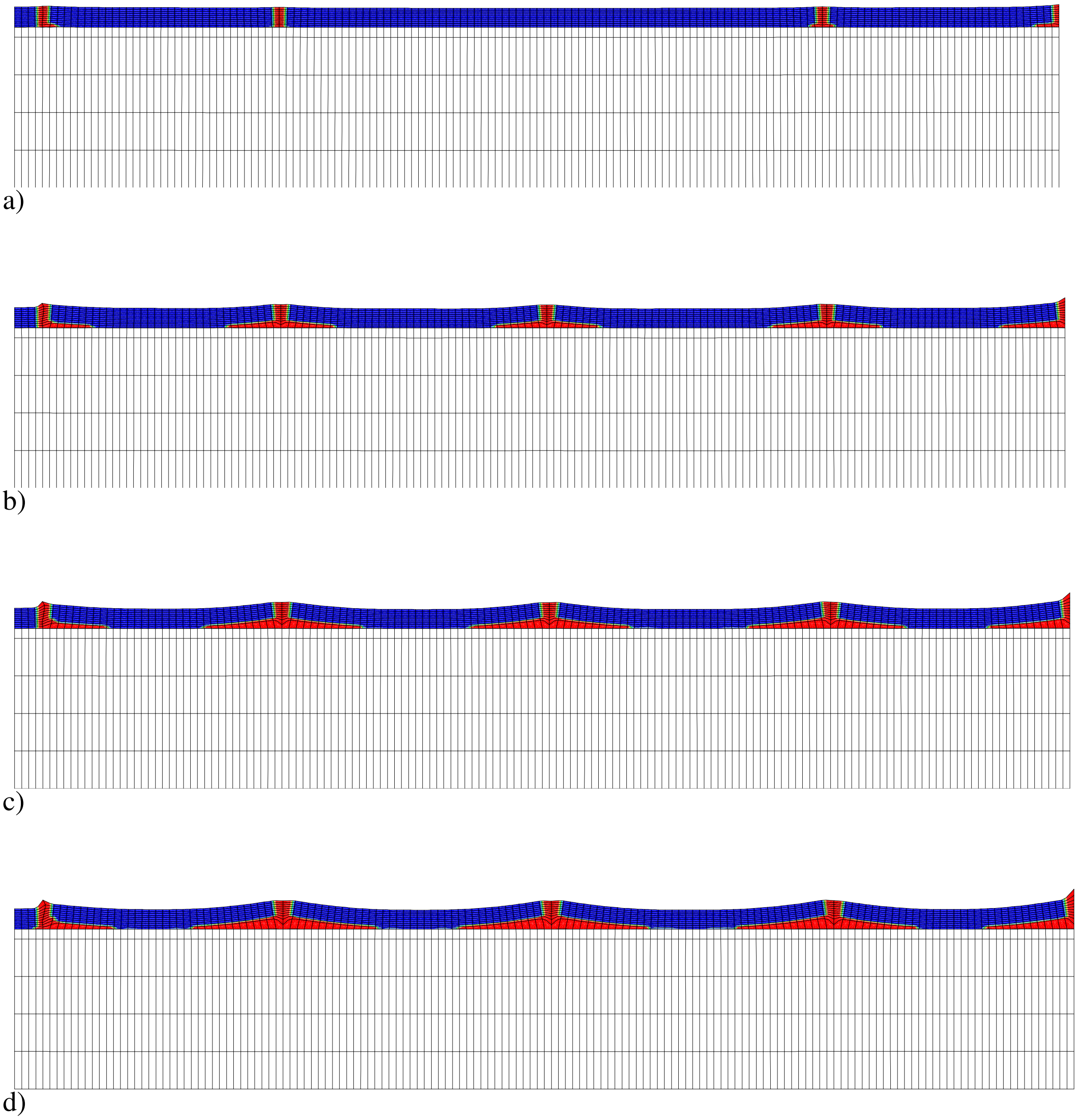

Figure 2: Damage distribution at the thin thermal coating for increasing loading stages from a) to d).

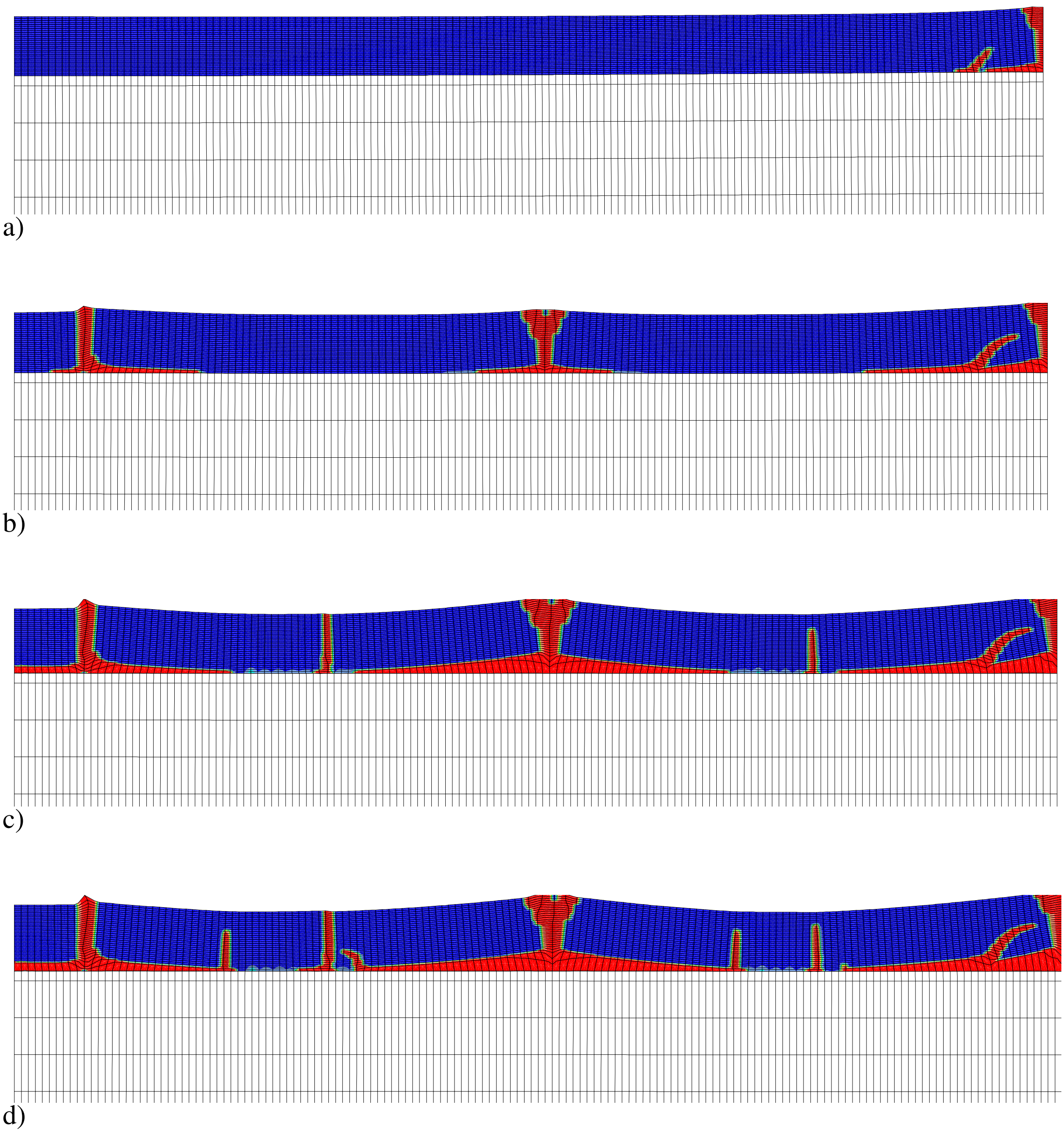

Figure 3: Damage distribution at the thin thermal coating for increasing loading stages from a) to d).

- Normal and tangential interface stiffness $K_n = K_t$ 50 kN/mm
- Fracture Energies $G_I = G_{II} =$ 0.3 N/mm
- Elastic normal traction limit $t_{0n} =$ 20 N.
- Friction coefficient and dilatancy coefficient $\alpha = \beta = 30^0$

The nonlinear Finite Element results related to a monotonic increasing loading are discussed in the following subsections. Two analysis are reported, with reference to the two different thickness.

3.1 Thin coating results

For the element with the thin coating of thickness $h_c^{(1)} =$ 0.2 mm, the results in terms of damage distribution at different loading levels are reported in Fig. 2. It emerges that after the formation of the first vertical crack in the coating, a second crack is formed at a distance $L_{(c)}$. Increasing the impressed displacement a further vertical crack is formed at mid distance $L_{(c)}/2$ between the previous two cracks. This development of vertical cracks ends with the formation and propagation of of delamination of the coating from the substrate which is the final condition of coating failure.

3.2 Thick coating results

For the element with a thicker coating, $h_{rc}^{(2)} =$ 0.6 mm, the results in terms of damage distribution at different loading levels are reported in Fig. 3. The scenario is now qualitatively different since, beside the same mechanism of vertical cracks which form at distance length multiple pair fraction of $L_{(c)}$, inclined cracks also develops. The inclined crack instead of starting from the external surface, the are originated at the bottom and then propagates up to the surface, or alternatively they reach one already developed vertical crack, inducing spallation of the coating. The competition in this case is among three mechanisms. Namely vertical cracks, inclined shear cracks and finally bottom delamination.

As final remark a well know design concept is confirmed by the numerical analises. Namely, a greater thickness is expected to give better thermal coating performance but it shows lower mechanical resistance. Therefore the optimal thickness has to be obtained by a compromise between thermal insulation performance and mechanical resistance.

Acknowledgments

The financial support of the Italian Ministry for University and Research (MIUR), under the grant PRIN-2015, project No. 2015LYYXA8. Multi-scale mechanical models for the design and optimization of micro-structured smart materials and metamaterials is gratefully acknowledged.

REFERENCES

[1] A.P. McGuigan, G.A.D. Briggs, V.M. Burlakov, M. Yanaka, Y. Tsukahara, An elastic-plastic shear lag model for fracture of layered coatings, *Thin Solid Films*, **424**, 219–223, 2003.

[2] Z.B. Chen, Z.G. Wang, S.J. Zhu, Tensile fracture behavior of thermal barrier coatings on superalloy, *Surf. Coatings Technol.*, **205**, 3931–3938 2011.

[3] J. Peng, F. Xueling, S. Yongle, L. Dingjun, W. Tiejun, Bending-driven failure mechanism and modelling of double-ceramic-layer thermal barrier coating system, *International Journal of Solids and Structures*, **130 131**, 11–20, 2018.

[4] R. Alessi, J. Ciambella, A. Paolone, Damage evolution and debonding in hybrid laminates with a cohesive interfacial law, *Meccanica*, **52**, 1079–1091, 2017.

[5] G. Borino, B. Failla, F. Parrinello, A symmetric nonlocal damage theory, *International Journal of Solids and Structures*, **40**, (13-14), 3621–3645, 2003.

[6] F. Parrinello, B. Failla, G., Borino, Cohesive-frictional interface constitutive model, *International Journal of Solids and Structures*, **46**, (13), 2680–2692 2009.

[7] F. Parrinello, G. Marannano, G. Borino, A. Pasta, Frictional effect in mode II delamination: Experimental test and numerical simulation, *Engineering Fracture Mechanics*, **110**, 258–269, 2013.

[8] F. Parrinello, G., Marannano, G. Borino, Mixed Mode Delamination Analysis by a Thermodynamically Consistent Cohesive Interface Model with Independent Mode i and Mode II Fracture Energies, *Procedia Engineering*, **109**, 327–337, 2015.

[9] F. Parrinello, G. Marannano, G. Borino, A thermodynamically consistent cohesive-frictional interface model for mixed mode delamination, *Engineering Fracture Mechanics*, **153**, 61–79, 2016.

[10] S. Marfia, E. Sacco, J. Toti, A coupled interface-body nonlocal damage model for the analysis of FRP strengthening detachment from cohesive material *Frattura ed Integrit Strutturale*, **18**, 23–33, 2011.

[11] M. Paggi, J. Reinoso, Revisiting the problem of a crack impinging on an interface:A modeling framework for the interaction between the phase field approach for brittle fracture and the interface cohesive zone model, *Computer Methods in Applied Mechanics and Engineering*, **321**, 145 – 172, 2017.

[12] Z.P. Bažant, M. Jirásek, Nonlocal integral formulations of plasticity and damage: Survey of progress, *Journal of Engineering Mechanics*, **128 (11)**, 1119–1149, 2002.

[13] B. Vandoren, A. Simone, Modeling and simulation of quasi-brittle failure with continuous anisotropic stress-based gradient-enhanced damage models, *Computer Methods in Applied Mechanics and Engineering*, **332**, 644–685, 2017.

[14] G. Giambanco, E. La Malfa Ribolla, A phase-field model for strain localization analysis in softening elastoplastic materials, *International Journal of Solids and Structures*, **172 - 173**, 84–96, 2019.

[15] W. Zhu, L. Yang, J.W. Guo, Y.C. Zhou, C. Lu, Determination of interfacial adhesion energies of thermal barrier coatings by compression test combined with a cohesive zone finite element model, *International Journal of Plasticity*, **64**, 76 – 87, 2015.

[16] G. Giambanco, G.F. Scimemi, A. Spada, The interphase finite element, *Computational Mechanics*, *50*, (3), 353–366, 2012.

[17] G.F. Scimemi, G. Giambanco, A. Spada, The interphase model applied to the analysis of masonry structures, *Computer Methods in Applied Mechanics and Engineering*, **279**, 66–85, 2014.

[18] R. Serpieri, G. Alfano, E. Sacco, A mixed-mode cohesive-zone model accounting for finite dilation and asperity degradation, *International Journal of Solids and Structures*, **67-68**, 102 – 115, 2015.

[19] C. Comi, U. Perego, Criteria for mesh refinement in nonlocal damage finite element analyses, *European Journal of Mechanics - A/Solids 23* (4), 615–623, 2004.

[20] F. Parrinello, G. Borino, Integration of finite displacement interface element in reference and current configurations, *Meccanica*, **53**, (6), 1455–1468, 2018.

[21] F. Parrinello, G. Borino, Non associative damage interface model for mixed mode delamination and frictional contact, *European Journal of Mechanics, A/Solids*, **76**, 108–122, 2019.